Developmental Cell
Article

Sensory Signaling-Dependent Remodeling of Olfactory Cilia Architecture in *C. elegans*

Saikat Mukhopadhyay,[1] Yun Lu,[2] Shai Shaham,[2] and Piali Sengupta[1,*]
[1]Department of Biology and National Center for Behavioral Genomics, Brandeis University, Waltham, MA 02454, USA
[2]Laboratory of Developmental Genetics, The Rockefeller University, New York, NY 10021, USA
*Correspondence: sengupta@brandeis.edu
DOI 10.1016/j.devcel.2008.03.002

SUMMARY

Nonmotile primary cilia are sensory organelles composed of a microtubular axoneme and a surrounding membrane sheath that houses signaling molecules. Optimal cellular function requires the precise regulation of axoneme assembly, membrane biogenesis, and signaling protein targeting and localization via as yet poorly understood mechanisms. Here, we show that sensory signaling is required to maintain the architecture of the specialized AWB olfactory neuron cilia in *C. elegans*. Decreased sensory signaling results in alteration of axoneme length and expansion of a membraneous structure, thereby altering the topological distribution of a subset of ciliary transmembrane signaling molecules. Signaling-regulated alteration of ciliary structures can be bypassed by modulation of intracellular cGMP or calcium levels and requires kinesin-II-driven intraflagellar transport (IFT), as well as BBS- and RAB8-related proteins. Our results suggest that compensatory mechanisms in response to altered levels of sensory activity modulate AWB cilia architecture, revealing remarkable plasticity in the regulation of cilia structure.

INTRODUCTION

Nonmotile primary cilia are microtubule-based sensory organelles that play critical roles in signal transduction (Scholey and Anderson, 2006; Singla and Reiter, 2006). Primary cilia consist of a central axoneme surrounded by a ciliary membrane that houses molecules such as receptors and channels required for sensation of environmental cues and signal transduction. Although the structures of many primary cilia are relatively simple, cilia present on sensory neurons can exhibit highly complex and diverse morphologies that are essential for their specialized functions. For example, vertebrate rods and cones exhibit highly elaborate outer segments that are unique ciliary structures consisting of membrane-associated molecules required for phototransduction. Ciliary dysfunction has been associated with a plethora of diseases (Bisgrove and Yost, 2006), indicating that maintenance of cellular homeostasis is critically dependent on efficient cilia activity. It is thus essential that the form and function of these structures are precisely regulated.

The elaboration of ciliary structures requires the coordination of axonemal shaft formation with ciliary membrane biogenesis (Sorokin, 1962). All cilia are formed via the highly conserved process of intraflagellar transport (IFT), which transports molecules essential for ciliary assembly and function (Rosenbaum and Witman, 2002; Scholey, 2003). IFT is mediated by the kinesin-2 and dynein molecular motors, which move cargo such as axoneme precursors in the anterograde and retrograde directions, respectively, as part of a highly conserved macromolecular protein complex referred to as the IFT particle (Cole et al., 1998; Kozminski et al., 1993). In addition to building the axoneme, IFT also plays a role in the targeting and movement of ciliary membrane proteins (Jenkins et al., 2006; Marszalek et al., 2000; Pan and Snell, 2003). The IFT20 protein is localized to the Golgi and has been implicated in the trafficking of ciliary membrane proteins from the Golgi to the cilia (Follit et al., 2006). IFT proteins are essential for Sonic hedgehog signaling in cilia (Corbit et al., 2005; Huangfu et al., 2003; May et al., 2005) and for adhesion-regulated activation of a membrane-localized kinase in the flagella of *Chlamydomonas* during mating (Wang et al., 2006). Another class of proteins also implicated in the regulation of cilia structure and function are the BBS proteins, and mutations in these proteins lead to the pleiotropic Bardet-Biedl syndrome (Ansley et al., 2003; Blacque et al., 2004). The BBS proteins have been suggested to coordinate the functions of kinesin-2 motors in the formation of the axoneme and in the assembly of IFT particles in *C. elegans* cilia (Blacque et al., 2004; Ou et al., 2005). Recently, the BBS protein complex has also been shown to regulate ciliogenesis in part via regulation of the small GTPase RAB8 (Nachury et al., 2007), which, in turn, regulates the targeting of transmembrane proteins to the cilia via post-Golgi vesicle fusion or exocytosis at the ciliary base (Moritz et al., 2001). Despite these findings, much remains to be understood regarding the coordination and regulation of IFT, ciliary membrane biogenesis, and signaling molecule localization in order to generate and maintain appropriate ciliary structures.

The nematode *C. elegans* is an excellent system in which to study the molecular mechanisms underlying cilia structure and function. *C. elegans* contains 60 ciliated neurons; of these, 12 pairs are located in the amphid chemosensory organs of the head (Perkins et al., 1986; Ward et al., 1975). Eight of these neuron pairs respond to different subsets of aqueous compounds and contain cilia with relatively simple structures (channel cilia) (Bargmann and Horvitz, 1991; Perkins et al., 1986; Ward et al., 1975). IFT can be observed and quantitated in real time in these cilia in vivo (Orozco et al., 1999), allowing for a detailed analysis and comparison of the process in both wild-type and mutant

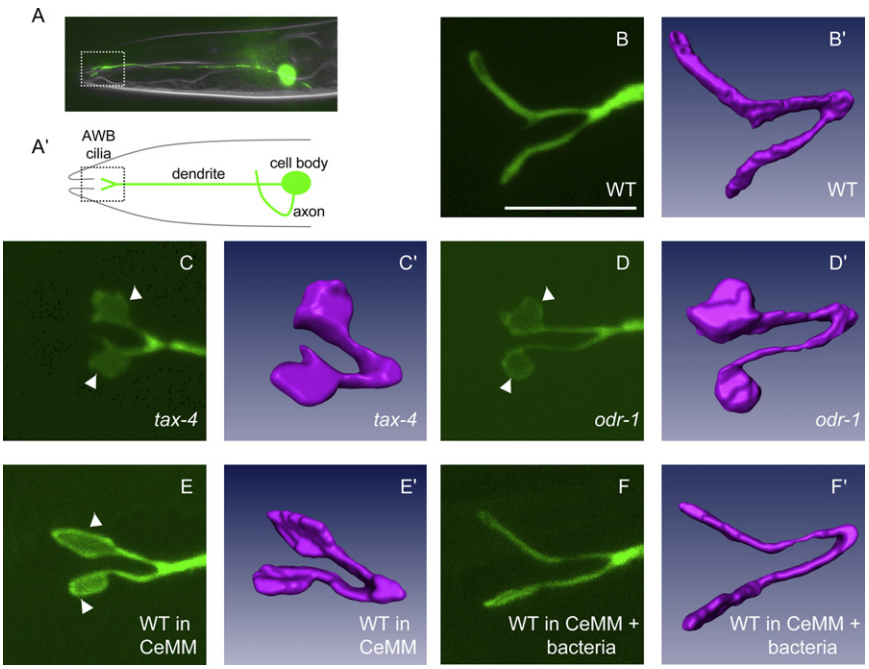

Figure 1. Sensory Signaling Modulates AWB Cilia Structure

(A and A′) Location of the cell body, processes, and cilia of an AWB olfactory neuron in the head of an adult animal. The AWB neuron is visualized via expression of *str-1::gfp*. Only one member of the bilateral AWB neuron pair is visible in the lateral view shown.

(B–F) The cilia of an AWB neuron visualized via *str-1p::gfp* transgene expression in (B and B′) wild-type (WT) adults grown under standard conditions, (C and C′) *tax-4(ks11)* adults, (D and D′) *odr-1 (n1936)* adults, (E and E′) wild-type adults grown in CeMM, and (F and F′) wild-type adults grown in CeMM + bacteria. All cilia images were acquired by using confocal microscopy.

(B′–F′) represent volumetric reconstructions from confocal projection series. Arrowheads indicate fans. Anterior is oriented toward the left in all images.

The scale bar is 7.5 μm for all confocal images.

animals. As is the case in other animals, formation of these cilia in *C. elegans* requires the kinesin and dynein motors, as well as highly conserved IFT particles and BBS proteins (Ansley et al., 2003; Blacque et al., 2004; Snow et al., 2004). The AWA, AWB, and AWC olfactory neurons respond to volatile odorants and contain highly elaborate and specialized cilia structures (wing cilia) (Bargmann et al., 1993; Perkins et al., 1986; Ward et al., 1975). These specialized cilia structures may be formed via cell-specific regulation of IFT (Evans et al., 2006; Mukhopadhyay et al., 2007). Both channel and wing cilia house transmembrane proteins required for sensory signal transduction, and a subset of these proteins is localized via IFT-dependent processes (Qin et al., 2005). The ability to manipulate the functions of defined sensory neurons in *C. elegans*, together with the ability to visualize the effects of these manipulations on individual cilia in vivo provides, an excellent opportunity to investigate the pathways and molecules required to generate and modulate neuron-specific ciliary structures.

Here, we show that sensory signal transduction is required to maintain, but not generate, the specialized ciliary structures of the AWB olfactory neurons in *C. elegans*. AWB cilia structure is similarly disrupted in wild-type animals grown in the absence of bacterial food-derived chemosensory cues, and in animals mutant for genes required for AWB-mediated sensory signal transduction. In particular, we find that membrane biogenesis is affected by levels of sensory signaling such that a membraneous structure is expanded and the distribution patterns of a subset of transmembrane signaling molecules is altered in response to decreased sensory signaling. These ciliary structural phenotypes can be bypassed via modulation of intracellular cGMP or calcium (Ca^{2+}) levels. We further demonstrate that sensory signaling-mediated structural remodeling requires kinesin-II-mediated IFT, as well as BBS- and RAB8-related proteins. Our results indicate that sensory signaling plays an active role in maintaining ciliary architecture and membrane protein localization in a specialized olfactory cilia type.

RESULTS

Mutations in Chemosensory Signal Transduction Molecules Alter AWB Olfactory Neuron Cilia Structure

To determine whether signaling genes known to be required for chemosensory signal transduction play a role in regulating cilia structure, we examined cilia in animals mutant for each of these molecules. Mutations in the *odr-3* $G\alpha_{i/o}$ subunit gene required for chemosensory signal transduction were previously shown to affect cilia structures of the AWA and AWC olfactory neurons (Roayaie et al., 1998). However, cilia of the AWA and AWC neurons exhibit complex, three-dimensional morphologies that are challenging to visualize and measure (Evans et al., 2006; Perkins et al., 1986). We therefore chose to focus on the cilia of the AWB neurons, which are relatively simpler structurally and which we have studied previously (Mukhopadhyay et al., 2007).

The cilia of the AWB neurons can be visualized via GFP expression driven by the AWB-specific *str-1* promoter (Mukhopadhyay et al., 2007; Troemel et al., 1997; Figures 1A and 1B). Although all AWB cilia in wild-type animals exhibit the characteristic Y-shaped structure, we observed animal-to-animal variability in both the lengths of each cilia branch and the area of a fan-shaped structure (henceforth referred to as a fan) occasionally present on either branch (Mukhopadhyay et al., 2007; Table 1). Dramatic and highly penetrant defects in AWB cilia structure were observed in animals mutant for the *odr-1* guanylyl cyclase, the *tax-2/tax-4* (*tax-2/4*) cyclic nucleotide-gated channel subunits, and the *grk-2* G protein-coupled receptor kinase genes (Figures 1C and 1D; Table 1). These molecules are expressed in, and required for, the sensory functions of the AWB neurons

Table 1. Sensory Signaling Regulates AWB Cilia Structure

Strain[a]	% Cilia with a Fan[b]	Median Fan Area/Cilia Branch in μm^2 (Q1, Q3)	Length of Long Cilia Branch ($\mu m \pm SD$)	Length of Short Cilia Branch ($\mu m \pm SD$)
Wild-type	51	0 (0, 0.5)	7.4 ± 1.1	5.9 ± 0.9
Wild-type in CeMM[c]	100[d]	3.0 (1.5, 4.6)[d]	6.5 ± 0.9[d]	5.2 ± 0.8[d]
Wild-type in CeMM[c] + bacteria	62	0 (0, 1.5)	7.3 ± 1.2	6.2 ± 1.1
Guanylyl cyclase mutants				
odr-1(n1936)	100[d]	3.2 (2.0, 4.1)[d]	6.5 ± 1.3[d]	4.9 ± 0.8[d]
odr-1(n1930)	100[d]	3.0 (2.0, 4.1)[d]	6.0 ± 0.7[d]	5.2 ± 0.4[d]
CNG-gated channel subunit mutants				
tax-2(p691)	100[d]	2.8 (1.5, 4.4)[d]	5.2 ± 1.1[d]	4.3 ± 0.9[d]
tax-2(p671)	95[d]	2.4 (0, 4.2)[d]	4.7 ± 1.2[d]	4.0 ± 0.5[d]
tax-2(ks31ts)	97[d]	2.2 (0.9, 3.5)[d]	5.3 ± 1.0[d]	4.3 ± 0.6[d]
tax-2(ks31ts); Ex[*str-1*p::*tax-2*::*gfp*]	67[e]	0 (0, 1.2)[e]	7.8 ± 1.1[e]	6.5 ± 1.1[e]
tax-4(p678)	100[d]	2.0 (1.1, 2.9)[d]	4.3 ± 0.4[d]	3.8 ± 0.3[d]
tax-4(ks11)	100[d]	2.9 (2.0, 4.0)[d]	4.6 ± 0.4[d]	3.9 ± 0.5[d]
tax-4(ks28)	100[d]	3.2 (2.2, 4.3)[d]	4.7 ± 0.6[d]	3.9 ± 0.5[d]
GPCR kinase mutants				
grk-2(gk268)	95[d]	2.1 (0, 3.2)[d]	6.8 ± 1.0	5.3 ± 0.9[d]
grk-2(rt97)	98[d]	2.5 (0.9, 3.2)[d]	6.3 ± 0.8[d]	4.8 ± 0.5[d]
grk-2(rt97); Ex[*str-1*p::*grk-2*]	52[f]	0 (0, 1.3)[f]	7.1 ± 1.0[f]	5.6 ± 0.9[f]
$G\alpha_{i/o}$ subunit mutants				
odr-3(n2150)	0[d]	0 (0, 0)[d]	6.5 ± 0.9[d]	4.6 ± 0.9[d]
odr-3(n1605)	2[d]	0 (0, 0)[d]	5.9 ± 0.9[d]	4.3 ± 0.9[d]
odr-3(Q206L)XS	0[d]	NA	2.3 ± 0.9[d]	1.9 ± 0.7[d]
Double/triple mutants				
odr-3(n2150); odr-1(n1936)	3	0 (0, 0)	5.6 ± 0.8[d]	4.3 ± 0.8[d]
odr-3(n2150); odr-1(n1936); Ex[*str-1*p::*odr-3*::*gfp*]	48[g]	0 (0, 2.1)[g]	ND	ND
tax-4(p678); odr-3(n2150)[h]	4	0 (0, 0)	5.7 ± 1.1[d]	4.2 ± 0.8[d]
tax-4(ks11); odr-3(n2150); odr-1(n1936)	5	0 (0, 0)	6.2 ± 0.8[d]	5.2 ± 0.8[d]

NA, not applicable; ND, not done; SD, standard deviation; Q1, 25th percentile; Q3, 75th percentile.
[a] The cilia of adult animals grown at 25°C were examined, except as indicated.
[b] A total of 20–145 cilia were examined for each.
[c] Animals were grown on CeMM agar plates at 20°C.
[d] Different from wild-type at $p < 0.001$.
[e] Different from *tax-2(ks31)* mutant animals at $p < 0.001$.
[f] Different from *grk-2(rt97)* mutant animals at $p < 0.001$.
[g] Different from *odr-3(n2150); odr-1(n1936)* mutant animals at $p < 0.001$.
[h] Animals were grown at 20°C.

(Coburn and Bargmann, 1996; Fukuto et al., 2004; Komatsu et al., 1996; L'Etoile and Bargmann, 2000). In *tax-2/4* mutants, the length of each ciliary branch was truncated, whereas the area of the fan was significantly increased (Figures 1C and 1C′; Table 1). In *odr-1* and *grk-2* mutants, we observed a similar increase in the area of the fan in all examined AWB cilia, with less severe changes in cilia branch lengths (Figures 1D and 1D′; Table 1). However, the overall surface area of the AWB cilia is not significantly altered in signaling mutants (total surface area: wild-type, 56.8 ± 8.6 μm^2 [n = 5]; *odr-1*, 47 ± 5.9 μm^2 [n = 5]; and *tax-4*, 57.5 ± 10.1 μm^2 [n = 4]). Similar phenotypes were observed in animals carrying different alleles of each gene (Table 1), as well as with *gfp* expressed under multiple AWB-selective promoters (data not shown). Expression of wild-type *tax-2* and *grk-2* cDNAs under the *str-1* promoter was sufficient to restore wild-type cilia morphology in *tax-2* and *grk-2* mutants, respectively (Table 1), indicating that these genes act cell autonomously to regulate AWB cilia structure. Although the ASI neurons also express these molecules (Komatsu et al., 1996; L'Etoile and Bargmann, 2000), we did not observe any ciliary defects in this neuron type (Table S1; see the Supplemental Data available with this article online).

The ODR-3 $G\alpha_{i/o}$ subunit has been suggested to transduce signals from ligand-bound receptors to the cGMP-mediated signaling pathway in *C. elegans* chemosensory neurons (Roayaie et al., 1998). However, loss-of-function (*lf*) mutations in *odr-3* caused a loss of all fan-like structures in examined cilia (Table 1), whereas overexpression of a constitutively active ODR-3

(*odr-3*(Q206L)XS) protein caused a marked shortening of the cilia branches (Table 1). Cilia phenotypes of animals doubly mutant for *odr-3(lf)* and *odr-1* or *tax-4* and animals of a *tax-4; odr-3; odr-1* triple mutant strain were similar to those of *odr-3(lf)* alone (Table 1), suggesting that ODR-3 either acts downstream of these molecules or in a parallel pathway. Taken together, these results indicate that mutations in a subset of AWB-expressed sensory signaling genes affect both AWB cilia branch length and shape.

AWB Ciliary Structures Are Altered in the Absence of Bacterial Food

Altered AWB ciliary structures in signaling mutants could arise as a consequence of compromised sensory signaling or, alternatively, due to sensory signaling-independent roles of these molecules in the regulation of ciliary architecture. To distinguish between these possibilities, we investigated whether AWB cilia structures are similarly altered in wild-type animals grown in the absence of bacterial food.

Olfactory neurons in *C. elegans* respond to chemicals produced by their bacterial food source (Bargmann et al., 1993). The AWB neurons have previously been shown to respond to the chemicals 2-nonanone and serrawettin W2, which are produced by pathogenic bacteria, and likely also mediate responses to additional bacteria-derived cues (Pradel et al., 2007; Troemel et al., 1997). We reasoned that growing animals in chemically defined axenic media (CeMM) in the absence of bacteria may decrease sensory signaling while simultaneously permitting growth and development, albeit at slower rates (Szewczyk et al., 2003, 2006).

We found that the AWB cilia of adult wild-type animals grown in either liquid or solid CeMM exhibited ciliary phenotypes similar to those observed in sensory signaling mutants (Figures 1E and 1E′; Table 1; Table S2). The observed ciliary phenotypes were likely not due to the altered metabolic rates and caloric restriction of CeMM-grown animals (Szewczyk et al., 2006), since no AWB ciliary phenotypes were observed in *eat-6(ad467)* Na^+/K^+ ATPase mutants, which also exhibit altered metabolic rates due to feeding defects (Avery, 1993; Davis et al., 1995; Lakowski and Hekimi, 1998; data not shown). Ciliary structural defects were suppressed when the CeMM was supplemented with bacteria (Figures 1F and 1F′; Table 1; Table S2). The AWB ciliary phenotypes of *odr-1* and *tax-4* mutants were not further altered upon cultivation in CeMM with or without bacteria (Table S2). Growth in CeMM also did not affect the ciliary structures of the ASH or ASI chemosensory neurons (Table S1). These results are consistent with the hypothesis that the AWB ciliary structures are altered to compensate for decreased sensory signaling, suggesting that the similar structural alterations observed in signaling mutants are due to altered sensory signal transduction and are not solely due to signaling-independent roles of these molecules in other cellular processes. However, it remains possible that CeMM is instructive for the formation of altered AWB ciliary structures, or that the expression or localization of one or more signaling gene is reduced upon growth in CeMM.

Ultrastructure of the AWB Cilia in Signaling Mutants

We previously described the ultrastructure of the wild-type AWB cilia, and we showed that the far-distal segments do not appear to contain an axoneme (Mukhopadhyay et al., 2007). We wished to determine whether the fan-shaped structures observed in sensory signaling mutants also lacked an axoneme and were perhaps membraneous extensions of the corresponding segments. Examination of serial sections of AWB cilia in *odr-1* and *tax-4* mutants via electron microscopy showed that, similar to wild-type animals, the middle segments of these cilia contained singlet and rare doublet microtubules, whereas rare singlet microtubules were present more distally (Movies S1–S3). The length of each cilia branch was truncated in *tax-4* mutants. In both *odr-1* and *tax-4* mutants, we observed a highly flattened structure corresponding to the fan at the distal segments of both cilia branches (Figures 2C and 2D). Three-dimensional reconstructions of the serial sections indicated that the fan structures are asymmetric, extending from each cilia branch in the direction away from the midline (Figure 2A). Similar structures were not observed in wild-type cilia grown under standard conditions (Figures 2A and 2B). The fan contained few, if any, singlet microtubules, which were generally restricted to the area proximal to the midline. Thus, mutations in *odr-1* and *tax-4* result in an altered membraneous structure at the distal segments of the AWB cilia. Examination of the micrographs did not reveal any structural alterations in channel cilia in signaling mutants (Figures 2C and 2D; Movies S2 and S3).

A Subset of Signal Transduction Molecules Is Localized to the Fan-Shaped Membraneous Areas

Signaling molecules such as receptors and channels are preferentially localized to the membranes of sensory cilia. We wished to determine whether the extended membraneous structures in CeMM-grown wild-type animals and in *odr-1* and *tax-4* signaling mutants also housed AWB-expressed transmembrane signal transduction molecules, or whether the composition of these areas was distinct.

To address this issue, we examined the localization of GFP-tagged ciliary transmembrane proteins, including the AWB-expressed STR-1 and SRD-23 chemoreceptors, TAX-2 and ODR-3. We verified that the tagged TAX-2 and ODR-3 proteins were functional by rescuing the AWB cilia defects in *tax-2* and *odr-3* mutants (Table 1), although no *str-1* or *srd-23* mutants are currently available. In wild-type or rescued animals grown under standard conditions, all GFP-tagged fusion proteins, with the exception of TAX-2, were localized throughout the AWB cilia, whereas TAX-2 was localized in a discrete proximal domain (Figures 3A–3D). In CeMM-grown wild-type animals and in *odr-1*, *tax-4*, and *grk-2* mutants, GFP-tagged STR-1, SRD-23, and ODR-3 fusion proteins were also present throughout the cilia, including in the fans (Figures 3A–3C). We did not observe any GFP-tagged TAX-2 protein in either *odr-1* or *tax-4* mutants, indicating that TAX-2 localization may depend on these genes (data not shown). Interestingly, however, TAX-2::GFP remained restricted to a proximal zone in *grk-2* mutants as well as in CeMM-grown wild-type animals, in a pattern similar to that in the cilia of wild-type animals grown in the presence of bacteria, and was excluded from the fan (Figure 3D). The localization of IFT particle and motor proteins such as OSM-6, OSM-3, and KAP-1 was also unaltered in signaling mutants, and these proteins were largely excluded from the membraneous expansions (Figure 3E; Figure S1). These results further indicate that the observed fans correspond to altered

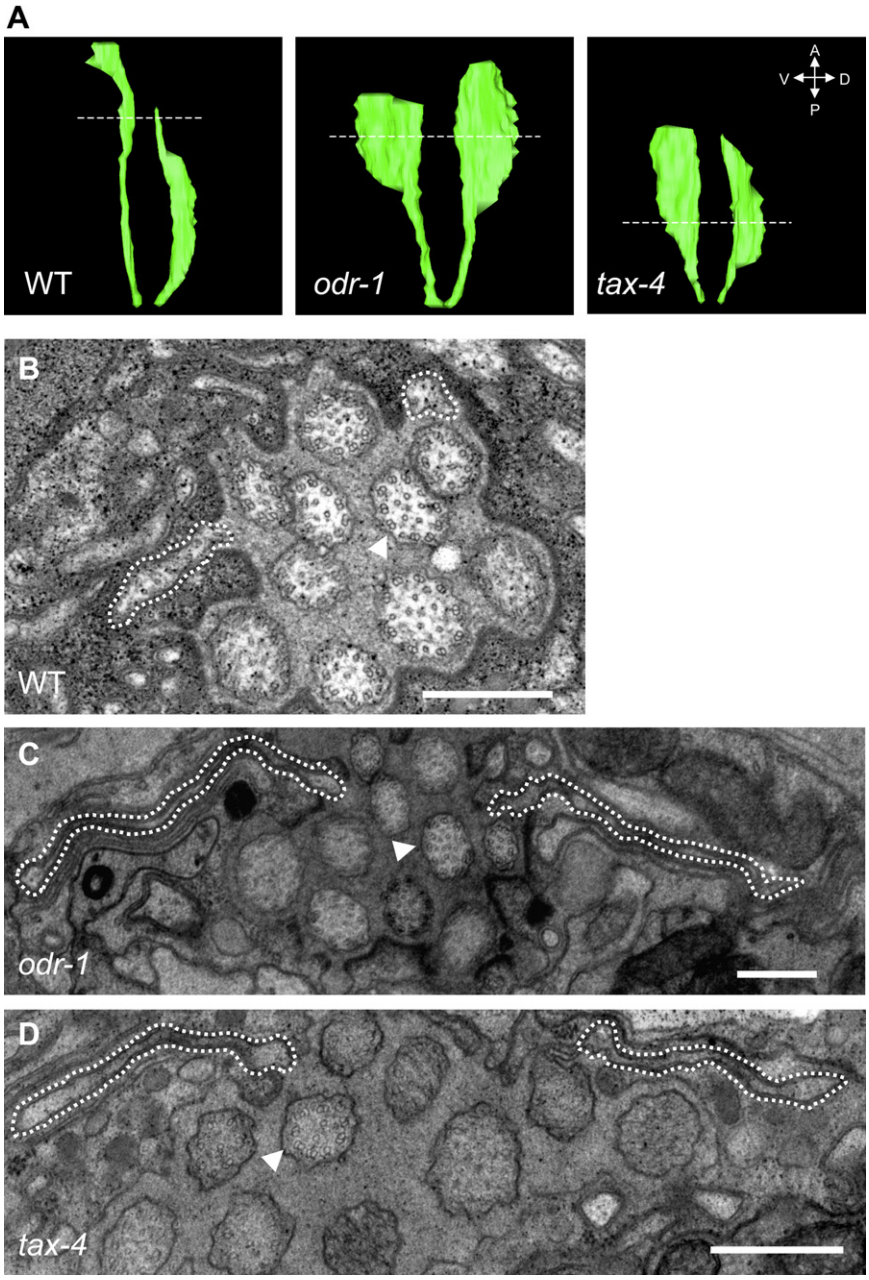

Figure 2. Ultrastructure of AWB Cilia in Signaling Mutants

(A) Three-dimensional reconstructions of the AWB cilia generated from serial EM sections obtained from wild-type, *odr-1(n1936)*, and *tax-4(ks11)* mutants. The broken lines indicate the sections shown in (B)–(D).

(B–D) A dashed line indicates the extent of the AWB cilia. Note that the axoneme structure of the channel cilia (one channel cilium is indicated by an arrowhead) is unaltered. The complete image sets of all acquired sections are shown in Movies S1–S3. The scale bars are 500 nm.

membrane structures, and that the overall distribution pattern of a subset of ciliary transmembrane signaling molecules is altered upon decreased sensory signaling (summarized in Figure 3F).

TAX-2 Acts during Postembryonic Development to Maintain AWB Cilia Structure

Cilia are formed during late embryonic development (Sulston et al., 1983). Sensory signaling may play a role in the generation or maintenance of these structures. To investigate the developmental stage at which sensory molecules are required to modulate AWB cilia architecture, we performed temperature-shift experiments with the temperature-sensitive *tax-2(ks31)* allele. The AWB cilia of *tax-2(ks31)* mutants exhibited wild-type morphology when animals were grown at the permissive temperature of 15°C, but exhibited large, fan-like structures and truncated branch lengths when grown at 25°C (Figures 4A–4D). We grew *tax-2(ks31)* animals at 15°C or 25°C and transferred them to 25°C or 15°C, respectively, at different larval stages. The structure of AWB cilia of adult animals moved from 25°C to 15°C at the L1 larval stage was similar to that of animals grown throughout their life cycle at 15°C, suggesting that the earlier embryonic phase of cilia development is not affected by mutations in *tax-2*. The AWB cilia of adult animals moved from 15°C to 25°C as late as the L4 larval stage also exhibited significantly aberrant morphology (Figures 4A–4D), indicating that TAX-2 function is required at late larval stages to maintain cilia architecture. Conversely, AWB cilia defects were decreased in animals moved from 25°C to 15°C at L2 and later larval stages (Figures 4A–4D). These results indicate that TAX-2 function is required during late larval stages to modulate AWB cilia morphology.

cGMP-Mediated Signaling Modulates Cilia Morphology

During chemosensory signal transduction, increased levels of cGMP generated by the guanylyl cyclase ODR-1 is thought to gate the TAX-2/4 channel (L'Etoile and Bargmann, 2000). Thus, in *odr-1* mutants, the TAX-2/4 channels may fail to open under appropriate conditions of sensory stimulation. If these molecules act similarly to regulate cilia architecture, then increasing cGMP levels in *odr-1*, but not *tax-4*, mutants may bypass the mutant phenotype. Addition of the membrane-permeable cGMP analog 8-Br-cGMP has previously been shown to bypass the phenotypes of the *daf-11* guanylyl cyclase mutant in the regulation of dauer formation (Birnby et al., 2000). We found that growing *odr-1(n1936)*, but not *tax-4(ks11)*, animals on plates containing 8-Br-cGMP partially suppressed the AWB cilia phenotypes (Figures 4E and 4F). Moreover, consistent with the finding that this pathway continues to act late in development to regulate cilia structure, addition of 8-Br-cGMP at later larval stages also

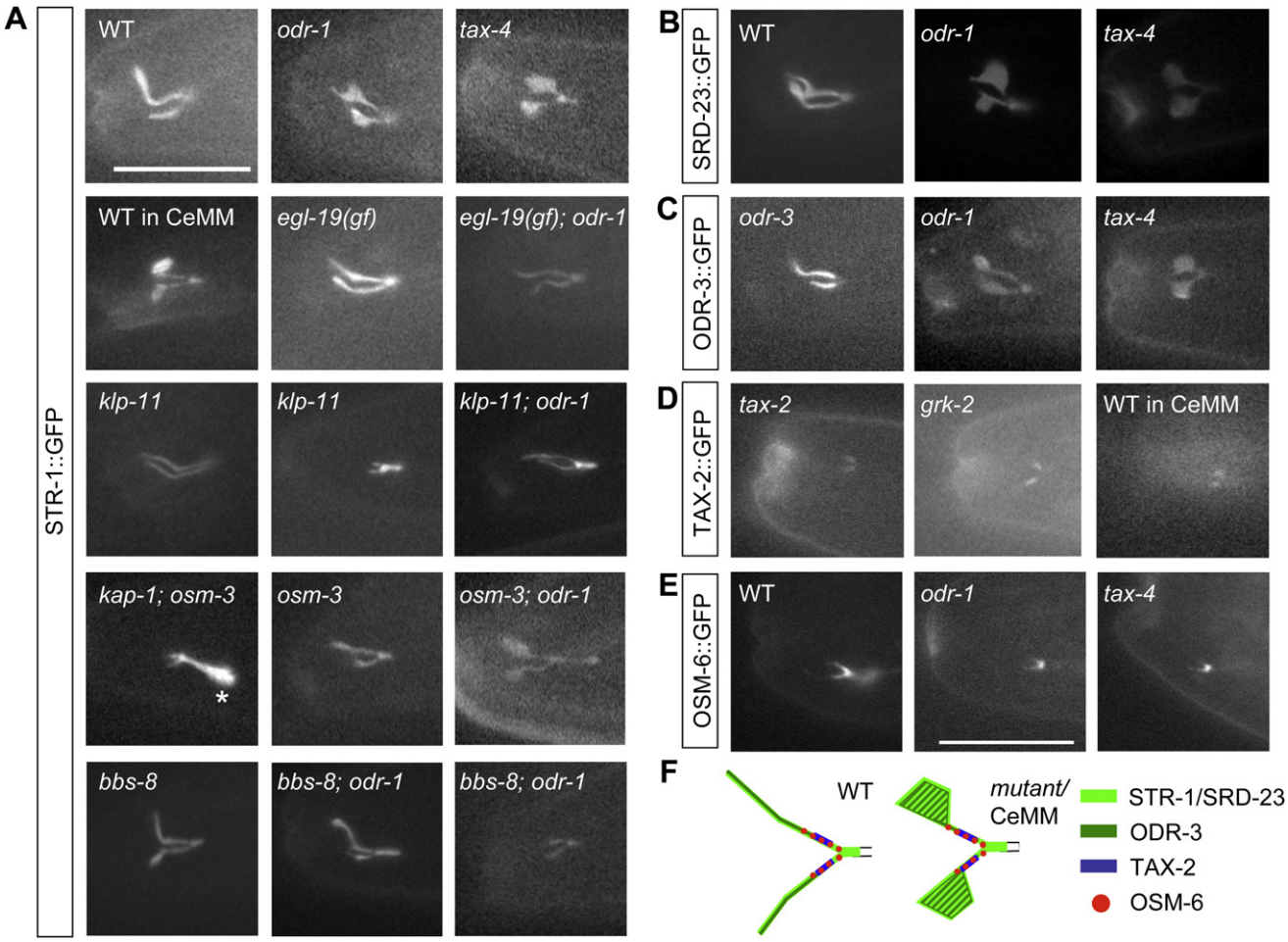

Figure 3. Localization of Ciliary Proteins in AWB Cilia

(A–E) Shown are the localization patterns of GFP-tagged (A) STR-1, (B) SRD-23, (C) ODR-3, (D) TAX-2, and (E) OSM-6 in the cilia of an AWB neuron in the indicated growth conditions and genetic backgrounds. For *klp-11* and *bbs-8; odr-1* mutants, the cilia branch length phenotypes exhibited by a subset of these animals are indicated in a second panel in (A). The asterisk in (A) indicates accumulation at the ciliary base in *kap-1; osm-3* double mutants. ODR-3::GFP and TAX-2::GFP rescue the corresponding mutant phenotypes, and their localization patterns in these mutant backgrounds are shown. OSM-6::GFP was previously shown to rescue the *osm-6* phenotype in the AWB neurons (Mukhopadhyay et al., 2007). Alleles used were *odr-1(n1936)*, *tax-4(ks11)*, *egl-19(n2368gf)*, *klp-11(tm324)*, *kap-1(ok676)*, *bbs-8(nx77)*, *osm-3(p802)*, and *grk-2(gk268)*. WT, wild-type. The scale bars are 15 μm.

(F) Summary of localization patterns of GFP-tagged proteins in AWB cilia.

resulted in significant rescue of the mutant phenotype (Figures 4E and 4F). Interestingly, addition of this cGMP analog also decreased both the percentage of cilia with fans, as well as the overall fan area of wild-type AWB cilia (Figures 4E and 4F), suggesting that growth of the fan is inversely correlated with intracellular cGMP levels.

Increased Calcium-Mediated Signaling Can Bypass the Cilia Defects of a Subset of Signaling Mutants

Gating of TAX-2/4 channels by cGMP is predicted to result in influx of cations such as Ca^{2+} (Kaupp and Seifert, 2002; Kimura et al., 2004). Mutations in *grk-2* have also been shown to decrease stimulus-evoked Ca^{2+} influx in the ASH sensory neurons (Fukuto et al., 2004). Thus, intracellular Ca^{2+} levels in the AWB neurons are predicted to be decreased in *odr-1*, *tax-2/4*, and *grk-2* mutants. We wondered if the defects in cilia architecture in these signaling mutants could be bypassed by increasing intracellular Ca^{2+} levels.

The L-type, voltage-gated Ca^{2+} channel *egl-19* is broadly expressed, including in neurons (Lee et al., 1997; data not shown). *gf* mutations in *egl-19* prolong the duration of depolarization (Avery, 1993; Lee et al., 1997; Raizen and Avery, 1994). *egl-19(gf)* mutations had minor effects on AWB cilia morphology on their own, but they strongly suppressed the cilia defects and the transmembrane protein localization phenotype of both *odr-1(n1936)* and *grk-2(gk268)* mutants (Figure 3A; Table S3). *lf* mutations in *egl-19* had minor effects on AWB cilia structures in either wild-type or mutant backgrounds (Table S3). *lf* mutations in the UNC-43 Ca^{2+}/calmodulin-dependent protein kinase II (CaMKII) (Reiner et al., 1999) alone also had minor effects on fan structure, but they did not further modify the *odr-1* cilia phenotype (Table S3). However, constitutively activated UNC-43

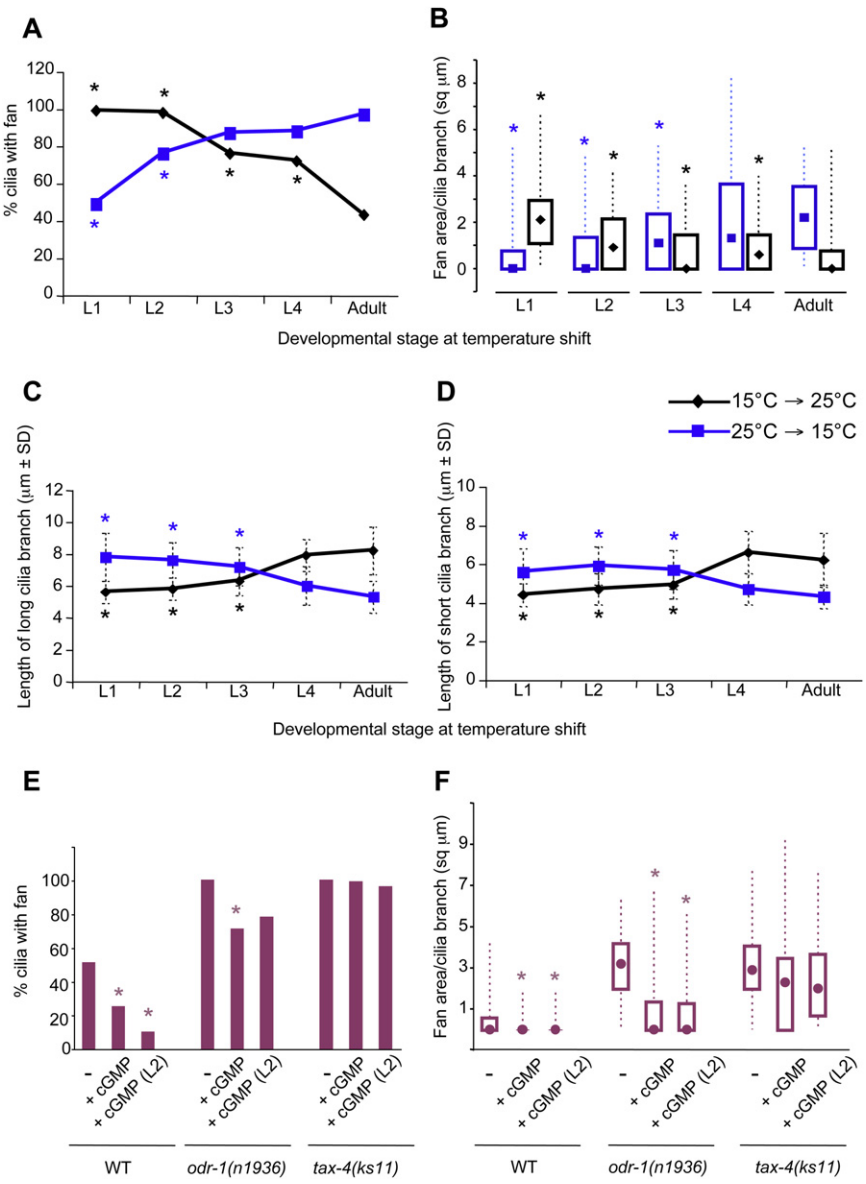

Figure 4. TAX-2 and ODR-1 Functions Are Required during Later Larval Stages to Modulate AWB Cilia Morphology

(A–D) *tax-2(ks31)* animals were raised at 15°C or 25°C and were shifted to 25°C or 15°C, respectively, at the indicated developmental stages. The (A) percentage of cilia exhibiting fans, the (B) fan area per cilia branch, and the lengths (±SD) of the (C) long and (D) short cilia branches were quantified. Asterisks mark values that are significantly different from those of animals grown throughout development at either 25°C (for animals shifted from 25°C to 15°C) or at 15°C (for animals shifted from 15°C to 25°C) at $p < 0.001$. n = 30–100 for each time point. Box plots in (B) show the 25th, 50th (median, represented by symbol), and 75th percentiles as well as the minimum and maximum values.

(E and F) Modulation of cGMP levels alters the AWB ciliary membrane area. Animals of the indicated genotypes were grown with or without 7 mM 8-Br-cGMP, and the (E) percentage of cilia with fans and the (F) fan areas were quantified. 8-Br-cGMP was present either throughout development or was added at the L2 larval stage. Shown are data from two or more independent experiments. Asterisks indicate values that are different from the corresponding strain grown in the absence of 8-Br-cGMP at $p < 0.001$. n = 30–200 for each. Box plots in (F) show the 25th, 50th (median, represented by filled circles), and 75th percentiles as well as the minimum and maximum values. All cilia measurements were performed in adult animals carrying stably integrated *str-1*p::*gfp* transgenes.

suppressed the *odr-1(n1936)* AWB cilia phenotype (Table S3). Neither *egl-19(gf)* or *unc-43(gf)* suppressed the cilia defects of *tax-4(ks11)* mutants (Table S3). These results suggest that increased Ca^{2+}-mediated signaling is partly sufficient to bypass the requirement for a subset of signaling molecules, but not that of the cyclic nucleotide-gated channel, in the regulation of AWB cilia structure.

Sensory Signaling-Mediated Remodeling of AWB Ciliary Architecture Requires Kinesin-II

We next investigated the mechanisms required for the signaling-mediated structural alterations in the AWB cilia. Formation of the fans and localization of transmembrane proteins to these structures may occur via diffusion after vesicle fusion at the cilia base, or may require active transport via IFT-dependent or IFT-independent mechanisms (Jenkins et al., 2006; Peden and Barr, 2005; Qin et al., 2005; Scholey and Anderson, 2006). We recently showed that the kinesin-II and OSM-3 anterograde motors act redundantly and independently of each other to form the AWB cilia middle segments, whereas neither motor appears to be essential to form the distal segments (Mukhopadhyay et al., 2007). This is in contrast to the functions of these motors in channel cilia in which both motors act cooperatively to form the middle segments, and OSM-3 alone acts to elongate the distal segments (Snow et al., 2004).

To determine whether IFT is altered in signaling mutants, we first investigated the movement of the IFT particle component OSM-6 as well as the KAP-1 kinesin-II and the OSM-3 motor subunits in the AWB cilia (Mukhopadhyay et al., 2007) of *odr-1*, *tax-4*, and *odr-3* mutants. Consistent with the localization of GFP-tagged IFT proteins and motors to the axoneme (Figure 3E), IFT could be observed only along the main cilia branches, and no IFT was observed in the fan-like structures (Figure S1; Movies S4–S6). The velocities and patterns of movement of GFP-tagged OSM-6 and kinesin motors in *odr-1, tax-4* and *odr-3* mutants were similar to those observed in wild-type AWB cilia (Table S4; Mukhopadhyay et al., 2007), indicating that IFT was not grossly altered by these mutations.

Table 2. Altered Cilia Structures Require Kinesin-II-Mediated Transport

Strain[a]	% Cilia with a Fan	Median Fan Area/Cilia Branch in μm^2 (Q1, Q3)[b]	Length of Long Cilia Branch (μm ± SD)	Length of Short Cilia Branch (μm ± SD)	% Lacking Cilia[c]
Wild-type[d]	51	0 (0, 0.5)	7.4 ± 1.1	5.9 ± 0.9	0
Wild-type in CeMM	97[e]	2.7 (1.7, 4.3)[e]	7.0 ± 0.9	5.8 ± 0.6	0
odr-1(n1936)[d]	100[e]	3.2 (2.0, 4.1)[e]	6.5 ± 1.3[e]	4.9 ± 0.8[e]	0
tax-4(ks11)[d]	100[e]	2.9 (2.0, 4.0)[e]	4.6 ± 0.4[e]	3.9 ± 0.5[e]	0
grk-2(gk268)[d]	95[e]	2.1 (0, 3.2)[e]	6.8 ± 1.0	5.3 ± 0.9[e]	0
Kinesin-II subunit mutants					
kap-1(ok676)	8[e]	0 (0, 0)[e]	6.9 ± 1.0	5.6 ± 1.0[e]	11
kap-1(ok676) in CeMM	51[f]	0 (0, 1.0)[f]	ND	ND	6
klp-11(tm324)	13[e]	0 (0, 0)[e]	6.7 ± 1.0[e]	5.2 ± 0.9[e]	17
klp-11(tm324) in CeMM	32[f]	0 (0, 0)[f]	ND	ND	7
kap-1(ok676); odr-1(n1936)	62[g]	0.7 (0, 1.9)[g]	ND	ND	13
kap-1(ok676); odr-1(n1936); Ex[*str-1*p::*kap-1::gfp*]	90	2.2 (0.5, 3.0)[h]	ND	ND	6
klp-11(tm324); odr-1(n1936)	45[g]	0 (0, 1.0)[g]	ND	ND	15
grk-2(gk268); klp-11(tm324)	31[i]	0 (0, 0)[i]	ND	ND	23
tax-4(ks11); klp-11(tm324)	35[j]	0 (0, 1.6)[j]	5.1 ± 0.9	4.3 ± 0.9	16
osm-3 mutants					
osm-3(p802)	59	0 (0, 0.7)	7.8 ± 1.1	6.4 ± 1.0	0
osm-3(p802); odr-1(n1936)	90[k]	3.0 (0, 4.0)[k]	ND	ND	0
grk-2(gk268); osm-3(p802)	85[k]	1.9 (0, 3.2)[k]	ND	ND	0
tax-4(ks11); osm-3(p802)	100[k]	2.9 (2.1, 4.0)[k]	4.9 ± 0.8[k]	4.1 ± 0.6[k]	0

[a] AWB cilia of adult animals grown at 25°C were examined, with the exception of CeMM (liquid)-cultivated animals, which were grown at 20°C. n = 25–150 for each.
[b] Severely truncated cilia were excluded.
[c] This category includes no cilia branches and severely truncated cilia (<1 μm), with occasional ectopic branches (Figure 3A).
[d] Data from Table 1.
[e] Different from wild-type at $p < 0.001$.
[f] Different from wild-type animals grown in CeMM at $p < 0.001$.
[g] Different from *odr-1(n1936)* mutant animals at $p < 0.001$.
[h] Different from *kap-1(ok676); odr-1(n1936)* mutant animals at $p < 0.001$.
[i] Different from *grk-2(gk268)* mutant animals at $p < 0.001$.
[j] Different from *tax-4(ks11)* mutant animals at $p < 0.001$.
[k] Not significantly different from corresponding *odr-1*, *grk-2*, or *tax-4* mutant animals.

We next determined whether formation of the fans requires IFT motor-based transport by examining the AWB cilia in CeMM-grown wild-type and signaling mutant animals lacking motor protein genes. Intriguingly, loss of function of either the *kap-1* or *klp-11* kinesin-II subunits alone resulted in a smaller fan in wild-type animals grown under standard conditions, and strongly suppressed the increased fan phenotypes in CeMM-grown wild-type animals, as well as in *odr-1*, *tax-4*, and *grk-2* mutants (Table 2). Correspondingly, the localization pattern of the STR-1::GFP fusion protein was also restored to the wild-type pattern (Figure 3A). This suppression was abolished upon expression of a wild-type *kap-1* cDNA, specifically in the AWB neurons (Table 2). However, the truncated cilia branch phenotype of *tax-4* mutants was not suppressed by mutations in kinesin-II subunits (Table 2), indicating that cilia membrane biogenesis and axoneme length may be regulated by distinct mechanisms. No suppression was observed in *osm-3* mutants (Figure 3A; Table 2). These results indicate that formation of the fans and the correlated localization pattern of transmembrane proteins upon reduction of sensory signaling requires kinesin-II-, but not OSM-3-mediated transport.

Since mutations in sensory signaling genes lead to ciliary structural phenotypes, the sensory behavioral defects exhibited by these mutants could be due to these ciliary defects. However, similar to what is seen with *odr-1* mutants, *klp-11; odr-1* double mutants failed to avoid the AWB-sensed volatile repellent 2-nonanone despite exhibiting wild-type ciliary morphology (Figure S2). Previously, defects in AWA- and AWC-mediated olfactory signaling in *odr-3* mutants were also suggested not to be caused by their ciliary defects (Lans et al., 2004). We could not examine the behaviors of wild-type animals grown in CeMM since these animals exhibited locomotory defects (S.M. and P.S., unpublished data). These observations suggest that the altered ciliary structures in signaling mutants may not directly contribute to sensory signaling defects, and that the behavioral defects of these mutants are likely due to their roles in sensory signal transduction. Interestingly, *klp-11* mutants exhibited weak defects in 2-nonanone avoidance (Figure S2), suggesting

Table 3. BBS Proteins and RAB-8/10 GTPases Modulate AWB Cilia Phenotypes of Signaling Mutants

Strain[a]	% Cilia with a Fan	Median Fan Area/Cilia Branch in μm^2 (Q1, Q3)	% Shortened Cilia[b]
Wild-type[c]	51	0 (0, 0.5)	0
odr-1(n1936)[c]	100[d]	3.2 (2.0, 4.1)[d]	0
tax-4(ks11)[c]	100[d]	2.9 (2.0, 4.0)[d]	0
BBS mutants			
bbs-1(ok1111)	52	0 (0, 0.5)	0
bbs-7(n1606)	37[d]	0 (0, 0.5)	29
bbs-8(nx77)	53	0 (0, 0.7)	2
bbs-1(ok1111); odr-1(n1936)	11[e]	0 (0, 0)[e]	67
bbs-7(n1606); odr-1(n1936)	21[e]	0 (0, 0.7)[e]	59
bbs-8(nx77); odr-1(n1936)	32[e]	0 (0, 0.9)[e]	41
RAB8-related mutants			
rab-8(tm2526)	25	0 (0, 0)	0
Ex[*str-1*p::*rab-8(Q67L XS)*]	0[d]	NA	92[f]
rab-8(tm2526); odr-1(n1936)	90	0.9 (0, 2.0)[e]	0
rab-8(tm2526); tax-4(ks-11)	88	0.9 (0, 1.8)[g]	0
rab-10(ok1494)[h]	79	0 (0, 1.2)	0
rab-10(ok1494); odr-1(n1936)[h]	33[e]	0 (0, 0)[e]	0
rab-10(ok1494); tax-4(ks11)[h]	84	0.8 (0, 1.6)[g]	9
arl-3 mutants			
arl-3(tm1703)	83[d]	0.8 (0, 1.5)[d]	0
arl-3(tm1703); odr-1(n1936)	100[i]	2.7 (1.7, 4.2)[i]	0
arl-3(tm1703); tax-4(ks-11)	100[i]	3.7 (2.6, 4.6)[i]	0

NA, not applicable.
[a] Cilia of adult animals grown at 25°C were examined. n = 50–120 for each.
[b] This category includes cilia with both branch lengths $\leq$ 4 μm and lacking a fan (Figure 3A; Figure S3D′). These cilia were excluded in the measurements of fan area.
[c] Data from Table 1.
[d] Different from wild-type at $p < 0.001$.
[e] Different from *odr-1(n1936)* mutant animals at $p < 0.001$.
[f] These cilia were severely truncated ($\leq$1 μm; Figure S3C). Similar effects of *rab-8[Q67L XS]* expression were observed in wild-type and *rab-8(tm2526)* mutant animals.
[g] Different from *tax-4(ks11)* mutant animals at $p < 0.001$.
[h] Animals were grown at 20°C.
[i] Not significantly different from corresponding *odr-1* or *tax-4* mutant animals.

that kinesin-II may play a role in the transport of signaling molecules in the AWB cilia, similar to previous observations in the AWC cilia (Evans et al., 2006) and in the flagella of *Chlamydomonas* (Pan and Snell, 2003).

BBS Proteins and RAB-8/10 Interact with the Sensory Signaling Pathway to Regulate AWB Cilia Structure

Recent work suggests that BBS proteins and RAB8 play a role in ciliary membrane biogenesis by facilitating docking and fusion of post-Golgi vesicles at the ciliary base (Moritz et al., 2001; Nachury et al., 2007). BBS proteins have also been suggested to couple the kinesin-II and OSM-3 motors to regulate ciliogenesis in *C. elegans* (Ou et al., 2005). The formation of a membraneous fan containing a subset of cilia-targeted transmembrane proteins in response to reduced sensory signaling, and the requirement of kinesin-II in this process, raised the possibility that BBS and/or RAB8 proteins may play a role in the formation of these altered structures. Homologs of many BBS proteins are encoded by the *C. elegans* genome (Blacque et al., 2004; Li et al., 2004; Ou et al., 2005). *C. elegans* RAB-8 and RAB-10 are related to mammalian RAB8 and play roles in vesicle trafficking and endocytic recycling, respectively, in nonneuronal tissues (Chen et al., 2006; Kamikura and Cooper, 2006). Both proteins are expressed broadly in *C. elegans*, including in neurons (Chen et al., 2006; S.M. and P.S. unpublished data).

Consistent with observations in channel cilia (Blacque et al., 2004), mutations in single *bbs* genes such as *bbs-7* caused truncated AWB cilia at a low penetrance, although no gross defects were observed in *bbs-8*, *bbs-1*, *rab-8*, and *rab-10* single mutants (Table 3; Figure S3). However, mutations in all three *bbs* genes, as well as in both *rab-8* and *rab-10*, suppressed the *odr-1* and *tax-4* phenotypes of the fan in the AWB cilia (Table 3; Figure S3). The area of STR-1::GFP localization corresponded to the area of the ciliary membrane in examined single and

double mutants (Figure 3A). *arl-3* also encodes a small GTPase and is expressed in ciliated neurons (Blacque et al., 2005). No suppression was observed upon loss of *arl-3* (Table 3), indicating the specific requirement for RAB-8/10 in this process. Surprisingly, animals doubly mutant for *odr-1* and all three *bbs* genes exhibited synergistic enhancement of the truncated AWB cilia phenotype (Table 3; Figure S3). Moreover, overexpression of a constitutively activated RAB-8 protein in the AWB neurons resulted in a loss of AWB ciliary branches (Table 3; Figure S3). These data imply that BBS- and RAB-8-related proteins are required for the formation of the membraneous fans and localization of transmembrane proteins to the fans in sensory signaling mutants. Moreover, both BBS proteins and RAB-8 may regulate axoneme length.

DISCUSSION

Our results indicate that sensory signal transduction is a critical regulator of AWB cilia architecture. Several lines of evidence are consistent with this hypothesis. First, we showed that molecules previously implicated in mediating sensory signal transduction in *C. elegans* as well as in more complex organisms also regulate AWB ciliary structure in a cell-autonomous manner. Second, the AWB ciliary structural phenotypes of signaling mutants could be phenocopied by growing wild-type animals in chemically defined media lacking bacterially derived chemosensory cues and could be suppressed upon the addition of bacteria. The formation of altered ciliary structures in both signaling mutants and food-deprived animals required kinesin-II function. Third, increasing levels of intracellular second messengers such as cGMP and Ca^{2+} required for sensory signal transduction were sufficient to bypass the AWB ciliary phenotypes of subsets of signaling mutants. Increased cGMP levels also suppressed fan formation in wild-type AWB cilia. Fourth, we found that the TAX-2 cyclic nucleotide-gated channel was required during late larval stages to maintain AWB ciliary morphology. TAX-2 has also previously been shown to act late in development to mediate sensory behaviors, and sensory activity has previously been implicated in the maintenance of correct axonal morphology of a subset of amphid sensory neurons (Coburn et al., 1998; Peckol et al., 1999). Taken together, these data suggest that the AWB neurons monitor sensory activity to regulate ciliary membrane biogenesis and axoneme length.

What are the mechanisms that translate levels of sensory signaling into remodeling of ciliary architecture? Activity-regulated ciliary remodeling requires kinesin-II, members of the BBS complex, and the small GTPases RAB-8 and RAB-10, which may act partly redundantly with each other. RAB8 is critical for vesicle trafficking from the trans-Golgi network to the plasma membrane, and it is required for the delivery of rhodopsin-containing vesicles to the base of the connecting cilium in photoreceptors (Deretic et al., 1995; Huber et al., 1993; Moritz et al., 2001; Nachury et al., 2007). Moreover, RAB8 enters and moves in the primary cilia of cultured cells (Nachury et al., 2007). Loss of RAB8 function diminishes ciliogenesis in primary cultured cells, whereas expression of a constitutively activated RAB8 results in increased cilia length (Nachury et al., 2007). However, we find that overexpression of a constitutively activated RAB-8 protein results in marked shortening of AWB cilia, suggesting that RAB-8 may inhibit cilia length but promote membrane biogenesis in AWB cilia. Kinesin-II, but not OSM-3, is also essential for activity-regulated modulation of AWB ciliary architecture, consistent with our previous findings that kinesin-II is the primary motor in AWB cilia (Mukhopadhyay et al., 2007). We did not observe any defects in the velocity of IFT motors or particles in the AWB cilia in signaling mutants, indicating that the core IFT process is unlikely to be affected upon reduction of sensory activity levels. In the simplest model, we suggest that reduced sensory activity (perhaps monitored via levels of intracellular cGMP or Ca^{2+}) increases RAB-8 and possibly RAB-10 functions, thereby altering the rate of vesicle trafficking to the plasma membrane, or the rate of vesicle docking and fusion at the ciliary base. Kinesin-II-mediated IFT may then transport these membrane-associated cargo into the cilia, resulting in modulation of membrane biogenesis. The BBS proteins may also play a role in this process by coupling the membrane to the IFT complex, or by regulating IFT particle assembly (Blacque et al., 2004; Ou et al., 2005).

What is the functional consequence of altering membrane architecture in response to sensory signaling? Reducing sensory activity results in expansion of the membraneous fans that contain subsets of signaling proteins. As a result, the overall layout of these molecules in the membrane is markedly distinct from that in wild-type cilia, which lack large fans. Although we are unable to determine whether the total number of protein molecules localized to the cilia is increased upon reduction of sensory activity, the more distributed localization of these molecules over the fan-like structure may enhance the olfactory receptivity and sensitivity of the AWB neurons (Takeuchi and Kurahashi, 2008). This enhancement may be necessary to compensate for decreased sensory signaling, thereby allowing animals to retain sensitivity to environmental signals. Altered trafficking and localization of ciliary membrane proteins may thus represent a homeostatic mechanism to maintain sensory activity levels. It is interesting to note that distribution of the TAX-2 channel is not regulated in a similar manner despite the predicted transmembrane topology of TAX-2, indicating that distribution of ciliary membrane proteins to the fan is not simply a passive process, but is highly regulated. A related mechanism has been proposed in "photostasis," by which rod photoreceptors alter their outer segment physiology and rhodopsin levels to compensate for their light environment. Thus, rats raised under dim (bright) light exhibited longer (shorter) outer segments and increased (decreased) rhodopsin levels (Penn and Williams, 1986; Williams et al., 1999). We speculate that the observed variability in AWB cilia structure in wild-type animals raised under standard conditions reflects animal-to-animal differences in sensory experiences.

Although we focus only on the cilia of the AWB neurons, the effects of activity are also detected on the maintenance of AWC olfactory neuron cilia (S.M. and P.S., unpublished data; Roayaie et al., 1998). Kinesin-II has also been suggested to play a role in the transport of sensory molecules to the AWC olfactory neuron cilia after ciliary assembly (Evans et al., 2006). However, no effects were observed on channel cilia. Expression of an activated G protein was shown to affect dye uptake by channel cilia, although no obvious structural abnormalities were detected (Zwaal et al., 1997). It is possible that these homeostatic mechanisms operate in only a subset of cell types, whose functions are critical to the survival of the animal. For example, the AWB

neurons mediate responses to chemicals produced by pathogenic bacteria (Pradel et al., 2007; Troemel et al., 1997), and loss or reduction of function of this important neuron type is likely to have severe consequences. Thus, it may be important for the animal to evolve regulatory mechanisms to maintain appropriate levels of AWB sensory function.

Taken together, we describe a remarkable degree of plasticity in cilia structure in *C. elegans*, which is likely to have important consequences on cellular function. This activity-regulated modulation of cilia architecture and protein localization bears striking resemblance to mechanisms regulating postsynaptic plasticity in the mammalian nervous system. Regulated trafficking of membrane proteins such as AMPA receptors and K^+ channels, as well as modulation of cellular morphology in response to synaptic activity, has been shown to underlie many aspects of neuronal plasticity and homeostasis (Collingridge et al., 2004; Turrigiano and Nelson, 2004; Kennedy and Ehlers, 2006). Similar to our observations regarding the requirement for RAB8 in membrane protein trafficking in the AWB cilia in sensory mutants, RAB8 has also been implicated in activity-regulated trafficking of AMPA receptors (Gerges et al., 2004). In addition, the morphology of neuronal structures such as dendritic spines are highly dynamic, are regulated by synaptic and sensory activity, and contribute to the modulation of neuron function (Alvarez and Sabatini, 2007). Thus, similar to the postsynapse, modulation of cilia structure and/or trafficking of membrane-localized signaling proteins in response to sensory activity may provide an effective mechanism by which cellular homeostasis is regulated and maintained. In this respect, the cilia may be considered postsynaptic to presynaptic environmental stimuli (Shaham, 2006). Given the critical role of cilia in the function of multiple cell types, it will be important to determine whether similar plasticity mechanisms operate to regulate cilia function and structural diversity in higher organisms.

EXPERIMENTAL PROCEDURES

Strain Construction

Strains were obtained from the *Caenorhabditis* Genetics Center, the National Bioresource Project (Japan), and Cori Bargmann. Stably integrated strains used in this work were: *kyIs104* (*str-1p::gfp*) (Troemel et al., 1997), *odr-3(Q206L)XS* (Roayaie et al., 1998), *oyIs14* (*sra-6p::gfp*) (Troemel et al., 1997), and *kyIs128 (str-3p::gfp*) (Peckol et al., 1999). Double or triple mutant strains were constructed by using standard methods.

Molecular Biology

str-1 promoter-driven cDNA constructs were generated by inserting 3 kb of *str-1* upstream regulatory sequences together with the respective cDNAs into *C. elegans* expression vectors. A subset of cDNAs was tagged with GFP-encoding sequences at their C-terminal ends. Full-length *gfp*-tagged *str-1* and *srd-23* fusion constructs have been described previously (Colosimo et al., 2004; Dwyer et al., 2001). The *gfp*-tagged *grk-2* construct and *grk-2* cDNA were obtained from D. Ferkey (Fukuto et al., 2004). *rab-8p::gfp* and *egl-19p::gfp* fusion constructs were generated by the PCR-fusion method (Hobert, 2002). All plasmids were verified by sequencing.

Transgenic strains were generated by injecting plasmids at 30 ng/μl, except for *str*-1 promoter-driven *gfp*-tagged *tax-2* and *odr-3* cDNAs and full-length *gfp*-tagged *str-1* and *srd-23* constructs, which were injected at 5 ng/μl. The *str-1p::rab-8(Q67LXS)* plasmid was injected at 100 ng/μl. *unc-122::dsRed* was used as the coinjection marker in all cases.

Microscopy

Images were acquired on a Zeiss Axioplan microscope equipped with a CCD camera (Hamamatsu). Fan area and cilia branch lengths were quantified by using OpenLab 4.0 software (Improvision).

Confocal images were acquired with a Leica spectral confocal microscope equipped with 63×/1.4 NA and 100×/1.4 NA objectives. Volumetric representations of cilia and calculations of total membrane surface area were performed by three-dimensional rendering of stacks of confocal images by using the Amira 4.1.1 graphics package.

Electron Microscopy

Adult hermaphrodites were fixed, stained, embedded in resin, and serially sectioned by using standard methods (Lundquist et al., 2001). Imaging was performed with an FEI Tecnai G2 Spirit BioTwin transmission electron microscope equipped with a Gatan 4K × 4K digital camera. Images of serial sections were processed, aligned, and modeled as surface renderings by using the IMOD 3.9.3 package (http://bio3d.colorado.edu/imod/; Kremer et al., 1996).

Growth in CeMM

Animals were cultured in CeMM media (generous gift of Nathaniel Szewczyk and Lewis Jacobson and custom made by Mediatech) according to previous protocols (Szewczyk et al., 2003). In brief, gravid animals from 2–3 6 cm NGM plates seeded with HB101 bacteria were bleached and washed in M9 buffer to release eggs and kill bacteria. Growth-synchronized, arrested L1 larvae were obtained by allowing these eggs to hatch by overnight incubation in M9 buffer. L1 larvae were then suspended in 1× CeMM liquid media or were cultured on CeMM plates containing 1.7% agar at 20°C in the dark. CeMM-cultured animals typically grew to the adult stage in 6–8 days.

Statistical Analyses

Analyses were performed by using the SPSS 13 statistical analyses package. Percentages were compared by using a chi-square test. Fan areas were compared by using a nonparametric independent sample Mann-Whitney U test for nonnormal distributions; cilia lengths were compared by using the independent sample t test.

SUPPLEMENTAL DATA

Supplemental Data include three figures, four tables, six movies, Supplemental Experimental Procedures, and Supplemental References and are available at http://www.developmentalcell.com/cgi/content/full/14/5/762/DC1/.

ACKNOWLEDGMENTS

We are grateful to Daniela Nicastro for assistance with three-dimensional reconstruction of EM sections; Kristin Ma for strain maintenance; Joel Rosenbaum for hosting S.M.; Michael Rosbash for access to a spinning disk confocal microscope; Don Katz for help with statistical analyses; Nathaniel Szewczyk and Lewis Jacobson for their generous gift of *C. elegans* axenic media and valuable advice on growth; and Cori Bargmann, Denise Ferkey, the *Caenorhabditis* Genetics Center, and Shohei Mitani at the National Bioresource Project (Japan) for strains. We also thank the Sengupta laboratory and Paul Garrity and the Garrity laboratory for discussions and comments on the manuscript. This work was supported by the National Institutes of Health (GM56223, P.S.; P30NS45713; and S10RR16708) and the National Science Foundation (DBI MRI 0722582). S.S. is a Klingenstein fellow in the Neurosciences and is a Monique Weill-Caulier Scholar.

Received: October 22, 2007
Revised: January 21, 2008
Accepted: March 3, 2008
Published: May 12, 2008

REFERENCES

Alvarez, V.A., and Sabatini, B.L. (2007). Anatomical and physiological plasticity of dendritic spines. Annu. Rev. Neurosci. *30*, 79–97.

Ansley, S.J., Badano, J.L., Blacque, O.E., Hill, J., Hoskins, B.E., Leitch, C.C., Kim, J.C., Ross, A.J., Eichers, E.R., Teslovich, T.M., et al. (2003). Basal body dysfunction is a likely cause of pleiotropic Bardet-Biedl syndrome. Nature *425*, 628–633.

Avery, L. (1993). The genetics of feeding in *Caenorhabditis elegans*. Genetics *133*, 897–917.

Bargmann, C.I., and Horvitz, H.R. (1991). Chemosensory neurons with overlapping functions direct chemotaxis to multiple chemicals in *C. elegans*. Neuron *7*, 729–742.

Bargmann, C.I., Hartwieg, E., and Horvitz, H.R. (1993). Odorant-selective genes and neurons mediate olfaction in *C. elegans*. Cell *74*, 515–527.

Birnby, D.A., Link, E.A., Vowels, J.J., Tian, H., Colacurcio, P.L., and Thomas, J.H. (2000). A transmembrane guanylyl cyclase (DAF-11) and Hsp90 (DAF-21) regulate a common set of chemosensory behaviors in *C. elegans*. Genetics *155*, 85–104.

Bisgrove, B.W., and Yost, H.J. (2006). The roles of cilia in developmental disorders and disease. Development *133*, 4131–4143.

Blacque, O.E., Reardon, M.J., Li, C., McCarthy, J., Mahjoub, M.R., Ansley, S.J., Badano, J.L., Mah, A.K., Beales, P.L., Davidson, W.S., et al. (2004). Loss of *C. elegans* BBS-7 and BBS-8 protein function results in cilia defects and compromised intraflagellar transport. Genes Dev. *18*, 1630–1642.

Blacque, O.E., Perens, E.A., Boroevich, K.A., Inglis, P.N., Li, C., Warner, A., Khattra, J., Holt, R.A., Ou, G., Mah, A.K., et al. (2005). Functional genomics of the cilium, a sensory organelle. Curr. Biol. *15*, 935–941.

Chen, C.C., Schweinsberg, P.J., Vashist, S., Mareiniss, D.P., Lambie, E.J., and Grant, B.D. (2006). RAB-10 is required for endocytic recycling in the *Caenorhabditis elegans* intestine. Mol. Biol. Cell *17*, 1286–1297.

Coburn, C.M., and Bargmann, C.I. (1996). A putative cyclic nucleotide-gated channel is required for sensory development and function in *C. elegans*. Neuron *17*, 695–706.

Coburn, C.M., Mori, I., Ohshima, Y., and Bargmann, C.I. (1998). A cyclic nucleotide-gated channel inhibits sensory axon outgrowth in larval and adult *Caenorhabditis elegans*: a distinct pathway for maintenance of sensory axon structure. Development *125*, 249–258.

Cole, D.G., Diener, D.R., Himelblau, A.L., Beech, P.L., Fuster, J.C., and Rosenbaum, J.L. (1998). *Chlamydomonas* kinesin-II-dependent intraflagellar transport (IFT): IFT particles contain proteins required for ciliary assembly in *Caenorhabditis elegans* sensory neurons. J. Cell Biol. *141*, 993–1008.

Collingridge, G.L., Isaac, J.T., and Wang, Y.T. (2004). Receptor trafficking and synaptic plasticity. Nat. Rev. Neurosci. *5*, 952–962.

Colosimo, M.E., Brown, A., Mukhopadhyay, S., Gabel, C., Lanjuin, A.E., Samuel, A.D., and Sengupta, P. (2004). Identification of thermosensory and olfactory neuron-specific genes via expression profiling of single neuron types. Curr. Biol. *14*, 2245–2251.

Corbit, K.C., Aanstad, P., Singla, V., Norman, A.R., Stainier, D.Y., and Reiter, J.F. (2005). Vertebrate Smoothened functions at the primary cilium. Nature *437*, 1018–1021.

Davis, M.W., Somerville, D., Lee, R.Y., Lockery, S., Avery, L., and Fambrough, D.M. (1995). Mutations in the *Caenorhabditis elegans* Na,K-ATPase α-subunit gene, *eat-6*, disrupt excitable cell function. J. Neurosci. *15*, 8408–8418.

Deretic, D., Huber, L.A., Ransom, N., Mancini, M., Simons, K., and Papermaster, D.S. (1995). *rab8* in retinal photoreceptors may participate in rhodopsin transport and in rod outer segment disk morphogenesis. J. Cell Sci. *108*, 215–224.

Dwyer, N.D., Adler, C.E., Crump, J.G., L'Etoile, N.D., and Bargmann, C.I. (2001). Polarized dendritic transport and the AP-1 μ1 clathrin adaptor UNC-101 localize odorant receptors to olfactory cilia. Neuron *31*, 277–287.

Evans, J.E., Snow, J.J., Gunnarson, A.L., Ou, G., Stahlberg, H., McDonald, K.L., and Scholey, J.M. (2006). Functional modulation of IFT kinesins extends the sensory repertoire of ciliated neurons in *Caenorhabditis elegans*. J. Cell Biol. *172*, 663–669.

Follit, J.A., Tuft, R.A., Fogarty, K.E., and Pazour, G.J. (2006). The intraflagellar transport protein IFT20 is associated with the Golgi complex and is required for cilia assembly. Mol. Biol. Cell *17*, 3781–3792.

Fukuto, H.S., Ferkey, D.M., Apicella, A.J., Lans, H., Sharmeen, T., Chen, W., Lefkowitz, R.J., Jansen, G., Schafer, W.R., and Hart, A.C. (2004). G protein-coupled receptor kinase function is essential for chemosensation in *C. elegans*. Neuron *42*, 581–593.

Gerges, N.Z., Backos, D.S., and Esteban, J.A. (2004). Local control of AMPA receptor trafficking at the postsynaptic terminal by a small GTPase of the Rab family. J. Biol. Chem. *279*, 43870–43878.

Hobert, O. (2002). PCR fusion-based approach to create reporter gene constructs for expression analysis in transgenic *C. elegans*. Biotechniques *32*, 728–730.

Huangfu, D., Liu, A., Rakeman, A.S., Murcia, N.S., Niswander, L., and Anderson, K.V. (2003). Hedgehog signalling in the mouse requires intraflagellar transport proteins. Nature *426*, 83–87.

Huber, L.A., Pimplikar, S., Parton, R.G., Virta, H., Zerial, M., and Simons, K. (1993). Rab8, a small GTPase involved in vesicular traffic between the TGN and the basolateral plasma membrane. J. Cell Biol. *123*, 35–45.

Jenkins, P.M., Hurd, T.W., Zhang, L., McEwen, D.P., Brown, R.L., Margolis, B., Verhey, K.J., and Martens, J.R. (2006). Ciliary targeting of olfactory CNG channels requires the CNGB1b subunit and the kinesin-2 motor protein, KIF17. Curr. Biol. *16*, 1211–1216.

Kamikura, D.M., and Cooper, J.A. (2006). Clathrin interaction and subcellular localization of Ce-DAB-1, an adaptor for protein secretion in *Caenorhabditis elegans*. Traffic *7*, 324–336.

Kaupp, U.B., and Seifert, R. (2002). Cyclic nucleotide-gated ion channels. Physiol. Rev. *82*, 769–824.

Kennedy, M.J., and Ehlers, M.D. (2006). Organelles and trafficking machinery for postsynaptic plasticity. Annu. Rev. Neurosci. *29*, 325–362.

Kimura, K.D., Miyawaki, A., Matsumoto, K., and Mori, I. (2004). The *C. elegans* thermosensory neuron AFD responds to warming. Curr. Biol. *14*, 1291–1295.

Komatsu, H., Mori, I., and Ohshima, Y. (1996). Mutations in a cyclic nucleotide-gated channel lead to abnormal thermosensation and chemosensation in *C. elegans*. Neuron *17*, 707–718.

Kozminski, K.G., Johnson, K.A., Forscher, P., and Rosenbaum, J.L. (1993). A motility in the eukaryotic flagellum unrelated to flagellar beating. Proc. Natl. Acad. Sci. USA *90*, 5519–5523.

Kremer, J.R., Mastronarde, D.N., and McIntosh, J.R. (1996). Computer visualization of three-dimensional image data using IMOD. J. Struct. Biol. *116*, 71–76.

L'Etoile, N.D., and Bargmann, C.I. (2000). Olfaction and odor discrimination are mediated by the *C. elegans* guanylyl cyclase ODR-1. Neuron *25*, 575–586.

Lakowski, B., and Hekimi, S. (1998). The genetics of caloric restriction in *Caenorhabditis elegans*. Proc. Natl. Acad. Sci. USA *95*, 13091–13096.

Lans, H., Rademakers, S., and Jansen, G. (2004). A network of stimulatory and inhibitory Gα-subunits regulates olfaction in *Caenorhabditis elegans*. Genetics *167*, 1677–1687.

Lee, R.Y., Lobel, L., Hengartner, M., Horvitz, H.R., and Avery, L. (1997). Mutations in the α1 subunit of an L-type voltage-activated Ca^{2+} channel cause myotonia in *Caenorhabditis elegans*. EMBO J. *16*, 6066–6076.

Li, J.B., Gerdes, J.M., Haycraft, C.J., Fan, Y., Teslovich, T.M., May-Simera, H., Li, H., Blacque, O.E., Li, L., Leitch, C.C., et al. (2004). Comparative genomics identifies a flagellar and basal body proteome that includes the BBS5 human disease gene. Cell *117*, 541–552.

Lundquist, E.A., Reddien, P.W., Hartwieg, E., Horvitz, H.R., and Bargmann, C.I. (2001). Three *C. elegans* Rac proteins and several alternative Rac regulators control axon guidance, cell migration and apoptotic cell phagocytosis. Development *128*, 4475–4488.

Marszalek, J.R., Liu, X., Roberts, E.A., Chui, D., Marth, J.D., Williams, D.S., and Goldstein, L.S. (2000). Genetic evidence for selective transport of opsin and arrestin by kinesin-II in mammalian photoreceptors. Cell *102*, 175–187.

May, S.R., Ashique, A.M., Karlen, M., Wang, B., Shen, Y., Zarbalis, K., Reiter, J., Ericson, J., and Peterson, A.S. (2005). Loss of the retrograde motor for IFT disrupts localization of Smo to cilia and prevents the expression of both activator and repressor functions of Gli. Dev. Biol. *287*, 378–389.

Moritz, O.L., Tam, B.M., Hurd, L.L., Peranen, J., Deretic, D., and Papermaster, D.S. (2001). Mutant rab8 impairs docking and fusion of rhodopsin-bearing post-Golgi membranes and causes cell death of transgenic *Xenopus* rods. Mol. Biol. Cell *12*, 2341–2351.

Mukhopadhyay, S., Lu, Y., Qin, H., Lanjuin, A., Shaham, S., and Sengupta, P. (2007). Distinct IFT mechanisms contribute to the generation of ciliary structural diversity in *C. elegans*. EMBO J. *26*, 2966–2980.

Nachury, M.V., Loktev, A.V., Zhang, Q., Westlake, C.J., Peranen, J., Merdes, A., Slusarski, D.C., Scheller, R.H., Bazan, J.F., Sheffield, V.C., et al. (2007). A core complex of BBS proteins cooperates with the GTPase Rab8 to promote ciliary membrane biogenesis. Cell *129*, 1201–1213.

Orozco, J.T., Wedaman, K.P., Signor, D., Brown, H., Rose, L., and Scholey, J.M. (1999). Movement of motor and cargo along cilia. Nature *398*, 674.

Ou, G., Blacque, O.E., Snow, J.J., Leroux, M.R., and Scholey, J.M. (2005). Functional coordination of intraflagellar transport motors. Nature *436*, 583–587.

Pan, J., and Snell, W.J. (2003). Kinesin II and regulated intraflagellar transport of *Chlamydomonas* aurora protein kinase. J. Cell Sci. *116*, 2179–2186.

Peckol, E.L., Zallen, J.A., Yarrow, J.C., and Bargmann, C.I. (1999). Sensory activity affects sensory axon development in *C. elegans*. Development *126*, 1891–1902.

Peden, E.M., and Barr, M.M. (2005). The KLP-6 kinesin is required for male mating behaviors and polycystin localization in *Caenorhabditis elegans*. Curr. Biol. *15*, 394–404.

Penn, J.S., and Williams, T.P. (1986). Photostasis: regulation of daily photon-catch by rat retinas in response to various cyclic illuminances. Exp. Eye Res. *43*, 915–928.

Perkins, L.A., Hedgecock, E.M., Thomson, J.N., and Culotti, J.G. (1986). Mutant sensory cilia in the nematode *Caenorhabditis elegans*. Dev. Biol. *117*, 456–487.

Pradel, E., Zhang, Y., Pujol, N., Matsuyama, T., Bargmann, C.I., and Ewbank, J.J. (2007). Detection and avoidance of a natural product from the pathogenic bacterium *Serratia marcescens* by *Caenorhabditis elegans*. Proc. Natl. Acad. Sci. USA *104*, 2295–2300.

Qin, H., Burnette, D.T., Bae, Y.K., Forscher, P., Barr, M.M., and Rosenbaum, J.L. (2005). Intraflagellar transport is required for the vectorial movement of TRPV channels in the ciliary membrane. Curr. Biol. *15*, 1695–1699.

Raizen, D.M., and Avery, L. (1994). Electrical activity and behavior in the pharynx of *Caenorhabditis elegans*. Neuron *12*, 483–495.

Reiner, D.J., Newton, E.M., Tian, H., and Thomas, J.H. (1999). Diverse behavioural defects caused by mutations in *Caenorhabditis elegans unc-43* CaM kinase II. Nature *402*, 199–203.

Roayaie, K., Crump, J.G., Sagasti, A., and Bargmann, C.I. (1998). The Ga protein ODR-3 mediates olfactory and nociceptive function and controls cilium morphogenesis in *C. elegans* olfactory neurons. Neuron *20*, 55–67.

Rosenbaum, J.L., and Witman, G.B. (2002). Intraflagellar transport. Nat. Rev. Mol. Cell Biol. *3*, 813–825.

Scholey, J.M. (2003). Intraflagellar transport. Annu. Rev. Cell Dev. Biol. *19*, 423–443.

Scholey, J.M., and Anderson, K.V. (2006). Intraflagellar transport and cilium-based signaling. Cell *125*, 439–442.

Shaham, S. (2006). Glia-neuron interactions in the nervous system of *Caenorhabditis elegans*. Curr. Opin. Neurobiol. *16*, 522–528.

Singla, V., and Reiter, J.F. (2006). The primary cilium as the cell's antenna: signaling at a sensory organelle. Science *313*, 629–633.

Snow, J.J., Ou, G., Gunnarson, A.L., Walker, M.R., Zhou, H.M., Brust-Mascher, I., and Scholey, J.M. (2004). Two anterograde intraflagellar transport motors cooperate to build sensory cilia on *C. elegans* neurons. Nat. Cell Biol. *6*, 1109–1113.

Sorokin, S. (1962). Centrioles and the formation of rudimentary cilia by fibroblasts and smooth muscle cells. J. Cell Biol. *15*, 363–377.

Sulston, J.E., Schierenberg, E., White, J.G., and Thomson, J.N. (1983). The embryonic cell lineage of the nematode *Caenorhabditis elegans*. Dev. Biol. *100*, 64–119.

Szewczyk, N.J., Kozak, E., and Conley, C.A. (2003). Chemically defined medium and *Caenorhabditis elegans*. BMC Biotechnol. *3*, 19.

Szewczyk, N.J., Udranszky, I.A., Kozak, E., Sunga, J., Kim, S.K., Jacobson, L.A., and Conley, C.A. (2006). Delayed development and lifespan extension as features of metabolic lifestyle alteration in *C. elegans* under dietary restriction. J. Exp. Biol. *209*, 4129–4139.

Takeuchi, H., and Kurahashi, T. (2008). Distribution, amplification and summation of cyclic nucleotide sensitivities within single olfactory sensory cilia. J. Neurosci. *28*, 766–775.

Troemel, E.R., Kimmel, B.E., and Bargmann, C.I. (1997). Reprogramming chemotaxis responses: sensory neurons define olfactory preferences in *C. elegans*. Cell *91*, 161–169.

Turrigiano, G.G., and Nelson, S.B. (2004). Homeostatic plasticity in the developing nervous system. Nat. Rev. Neurosci. *5*, 97–107.

Wang, Q., Pan, J., and Snell, W.J. (2006). Intraflagellar transport particles participate directly in cilium-generated signaling in *Chlamydomonas*. Cell *125*, 549–562.

Ward, S., Thomson, N., White, J.G., and Brenner, S. (1975). Electron microscopical reconstruction of the anterior sensory anatomy of the nematode *Caenorhabditis elegans*. J. Comp. Neurol. *160*, 313–337.

Williams, T.P., Squitieri, A., Henderson, R.P., and Webbers, J.P. (1999). Reciprocity between light intensity and rhodopsin concentration across the rat retina. J. Physiol. *516*, 869–874.

Zwaal, R.R., Mendel, J.E., Sternberg, P.W., and Plasterk, R.H. (1997). Two neuronal G proteins are involved in chemosensation of the *Caenorhabditis elegans* dauer-inducing pheromone. Genetics *145*, 715–727.